The orientation of the Seyfert nucleus in Markarian 348

S. Antón^{1,3*}, A.H.C. Thean^{1,2}, A. Pedlar¹, I.W.A. Browne¹

- ¹ Jodrell Bank Observatory, University of Manchester, U.K.
- ² Istituto di Radioastronomia-CNR, Bologna, Italy
- ³ CAAUL, Observatório Astronómico de Lisboa, Portugal

8 November 2018

ABSTRACT

Multi-frequency observations of Mrk 348 are presented consisting of 2 epochs of MERLIN data at 5 GHz, ISOPHOT data at 170, 90, 60 and 25 μ m, NOT images at U, B, R and I bands and data at 1350 μ m from the archive for SCUBA. The new optical images reveal a disrupted arm that ends towards the eastern companion of Mrk 348, consistent with the hypothesis that Mrk 348 and its companion form an interacting system. 5 GHz MERLIN imaging shows that only one of the radio components of Mrk 348 is polarized (%P=5). The broadband spectrum of Mrk 348 is flat between the radio and millimetre bands, suggesting that synchrotron emission extends to high frequencies. Mrk 348 has many of the characteristics of a radio-loud object. We discuss the orientation of the radio axis of Mrk 348 with respect to the line of sight. We conclude that the evidence is conflicting, and the geometry in Mrk 348 is not well-described by a simple edge-on or face-on model.

Key words: galaxies: active - galaxies: individual: (Mrk 348) - galaxies: interactions - galaxies: jets - galaxies: photometry - infrared: galaxies - radio continuum: galaxies - polarization.

INTRODUCTION

Active Galactic Nuclei (AGN) are thought of as existing in broadly two flavours: those with strong radio emission, the "radio-loud", and those with weaker radio emission, the "radio-quiet". There is strong evidence that radio-loud AGNs are hosted by elliptical galaxies, whereas radio-quiet AGNs, at least those of low redshift, are mainly found in spiral galaxies. Recently, however, the difference between radio-loud objects and radio-quiet has been blurred by results that show that at high redshift (and high luminosity) the hosts of radio-quiet quasars are ellipticals too † (e.g. McLure et al. 1999). Apart from radio emission (and related non-thermal emission at other wavelengths), there is almost no difference between radio-quiet and radio-loud sources of the same optical spectroscopic type.

Mrk 348 (B0046+316) is a relatively nearby (z=0.015) bright Seyfert 2 galaxy (R=13 mag) that has been extensively studied. The optical total intensity spectrum of Mrk348 shows narrow emission lines (e.g. Marchã et al. 1996) while spec-

tropolarimetric observations reveal a hidden broad line region (Tran 1995, Miller & Goodrich 1990). Observed by the VLA[‡] in A configuration at 8.4 GHz, Mrk348 has a core-dominated unresolved radio morphology (Wilkinson et al. 1998). At 5 GHz the radio nucleus of Mrk348 at VLBI§ resolution has a linear triple structure with 0.2" size at a $PA=168^{\circ}$ (Neff & De Bruyn 1983). Capetti et al. (1996) detected [OIII] emission confined in a linear structure with 0.45" size that aligns very well with the triple radio structure. Also, Falcke et al. (1998) found that the emission-line region is very concentrated within the central arcsecond. MERLIN[¶] observations show that the central component of the triple has an inverted radio spectrum, suggesting it is the core (Unger et al. 1984). Flux density monitoring shows that the core is variable at 5 GHz on scales of months (Neff & De Bruyn 1983). At 15 GHz and with the VLBA resolution of \sim 1 mas, Mrk 348 shows a one sided core-jet structure (Ulvestad et al. 1999; hereafter U99). The comparison of two epochs of VLBA observations suggests that the radio com-

^{*} Guest User, Canadian Astronomy Data Center, which is operated by the Dominion Astrophysical Observatory for the National Research Council of Canada's Herzberg Institute of Astrophysics.
† Apart from few exceptions (e.g. III Zw 2), powerful radio-quiet AGNs have not been detected in spiral galaxies.

[‡] Very Large Array

[§] Very Long Baseline Interferometry

 $[\]P$ Multi Element Radio Linked Interferometer Network

^{||} Very Long Baseline Array

ponents are expanding with sub-relativistic speeds (U99). Between 1997.1 and 1998.75 the core has undergone a major radio flare, increasing by a factor of 5.5 in flux density (U99). Ginga observations of Mrk 348 reveal a hard X-ray component, which is absorbed at low energies; the estimated line-of-sight column density is $n_H \sim 10^{23.1} {\rm cm}^{-2}$ (e.g. Warwick et al. 1989). Recently Falcke et al. (2000) reported the detection of an H₂O megamaser in Mrk 348.

Mrk 348 has been usually discussed in studies concerning the properties of Seyfert galaxies, which are mainly radioquiet objects. However, the radio properties of Mrk 348 are comparable with those of low-luminosity radio-loud objects. Mrk 348 challenges the standard radio-loud/radio-quiet picture in that it is a relatively strong radio emitter but it is hosted by a spiral galaxy. Some of the properties of Mrk 348 are very similar to those of III Zw 2, a Seyfert I galaxy in which superluminal motion has recently been detected (Brunthaler et al. 2000). Even though no superluminal motion has been observed in Mrk 348, its properties fit nicely the expectation for a radio-intermediate quasar (as it is the case of III Zw 2), of the kind suggested by Falcke et al. (1996). In this scenario the objects are intrinsically weak radio emitters but, due to relativistic boosting, their radio emission is amplified.

We have been gathering new data on Mrk 348, which are presented and discussed in this paper. The new set of observations comprise multi-frequency data from the radio to the optical band. There are 2 epochs of MERLIN data at 5 GHz, ISOPHOT** data at 170, 90, 60 and 25 μ m, and high (ground-based telescope) resolution NOT^{††} images at U, B, R and I bands. We also present data at $1350\mu m$ from the JCMT^{‡‡} archive for SCUBA^{§§}. In this paper we discuss the host galaxy of Mrk 348, the spectral energy distribution (SED) of its nuclear emission and the polarization at 5 GHz. Based on the available information, we discuss the orientation of the radio axis of Mrk 348 with respect to the line of sight. The paper is organised as follows: in Section 2 the multi-frequency observations and data reduction are presented, in Section 3 both the large-scale properties and the central region properties of Mrk 348 are discussed. In Section 4 we discuss the radio-loudness of Mrk 348, including the orientation of the radio emission with respect to the line of sight. The important points of this work are summarised in Section 5. Throughout the paper we assume $H_o = 65 \text{kms}^{-1} \text{Mpc}^{-1} \text{ and } q_o = 0.$

2 OBSERVATIONS AND DATA REDUCTION

2.1 MERLIN data

We obtained MERLIN 5–GHz images of Markarian 348 on two occasions. The first observing run took place on the 14th of December 1992, the second on the 10th of November 1998. A bandwidth of 15 MHz, centred at 4993 MHz, with both

right and left polarisation, was used. Flux density calibration was carried out using 3C 286 and relative baseline gains were determined by observing OQ 208. For each run, the data were phase calibrated using different nearby calibrators; 0103+337 (1992 observations) and 0052+298 (1998 observations). In order to register images from the two epochs we have introduced a +0.1398 arcsec shift in RA to the 1992 data (the difference in position between the positions of the southern component in the uniform maps); the position assumed for 0052+298 (α_{J2000} =00h 54m 45.88973s, δ_{J2000} = $30^{\circ} \ 06' \ 58.3828''$), as taken from Wilkinson et al. (1998), is probably more reliable than that assumed for 0103+337 $(\alpha_{J2000} = 01\text{h }06\text{m }00.28710\text{s}, \ \delta_{J2000} = 34^{\circ} \ 02' \ 03.0392'').$ The data were subjected to several passes of self-calibration. The resulting data were Fourier-transformed to a 0.015 arcsec grid resulting in angular resolutions of: a) 1992 epoch -73x54 mas using a natural-weighting scheme and 44x35 mas using a uniform-weighting scheme b) 1998 epoch - 72x51 mas using a natural weighting-scheme and 58x37 mas using a uniform-weighting scheme.

Naturally-weighted and uniformly-weighted contour maps of the source at the two epochs are presented in Figure 1. Flux densities were determined using the AIPS task TV-STAT and the positions measured using JMFIT. The flux densities and positions derived from the uniform images are given in Table 1. The 1992 and 1998 measurements are consistent with each other within the errors, although the flux density of the central component has varied by approximately a factor of two. The relative positions of the components at the two epochs agree within 5 mas. The images are consistent with the lower resolution (70 mas) early MERLIN results at 5 GHz (Unger et al. 1984) and the VLBI measurements of Neff & deBruyn (1983).

The images were calibrated for polarisation using 3C 286; the polarisation vectors are shown in Figure 1. Only the southern component shows significant polarisation and the direction of the polarisation vectors are approximately North-South. The polarized flux density of the southern component was 2.5 mJy and 3 mJy in the 1992 and 1998 data sets respectively. When noise and sources of calibration errors are taken into account the increase in polarised flux is not significant. Hence the southern component is \sim 5% polarised, whereas the stronger central component shows no polarisation greater than 1 mJy (<0.5%).

2.2 SCUBA - Data from Archive

Mrk 348 was observed at the JCMT with SCUBA at 1350 μ m and we retrieved the data from the archive. The data were processed with the SURF (SCUBA User Reduction Facility) package. The reduction process was based in the techniques described in Stevens et al. (1997), which includes the nod compensation, flatfielding, correction for extinction and flux density calibration.

We obtained a value for the flux density at 1350 μm of 187 \pm 8 mJy, the error on the flux density includes the calibration uncertainties and the instrumental flux uncertainties, added in quadrature.

 $^{^{\}star\star}$ ISOPHOT, one of the 4 instruments on board of the Infrared Space Observatory (ISO)

^{††} Nordic Optical Telescope

^{‡‡} the James Clerk Maxwell Telescope

^{§§} Submillimetre Common-User Bolometer Array on the JCMT.

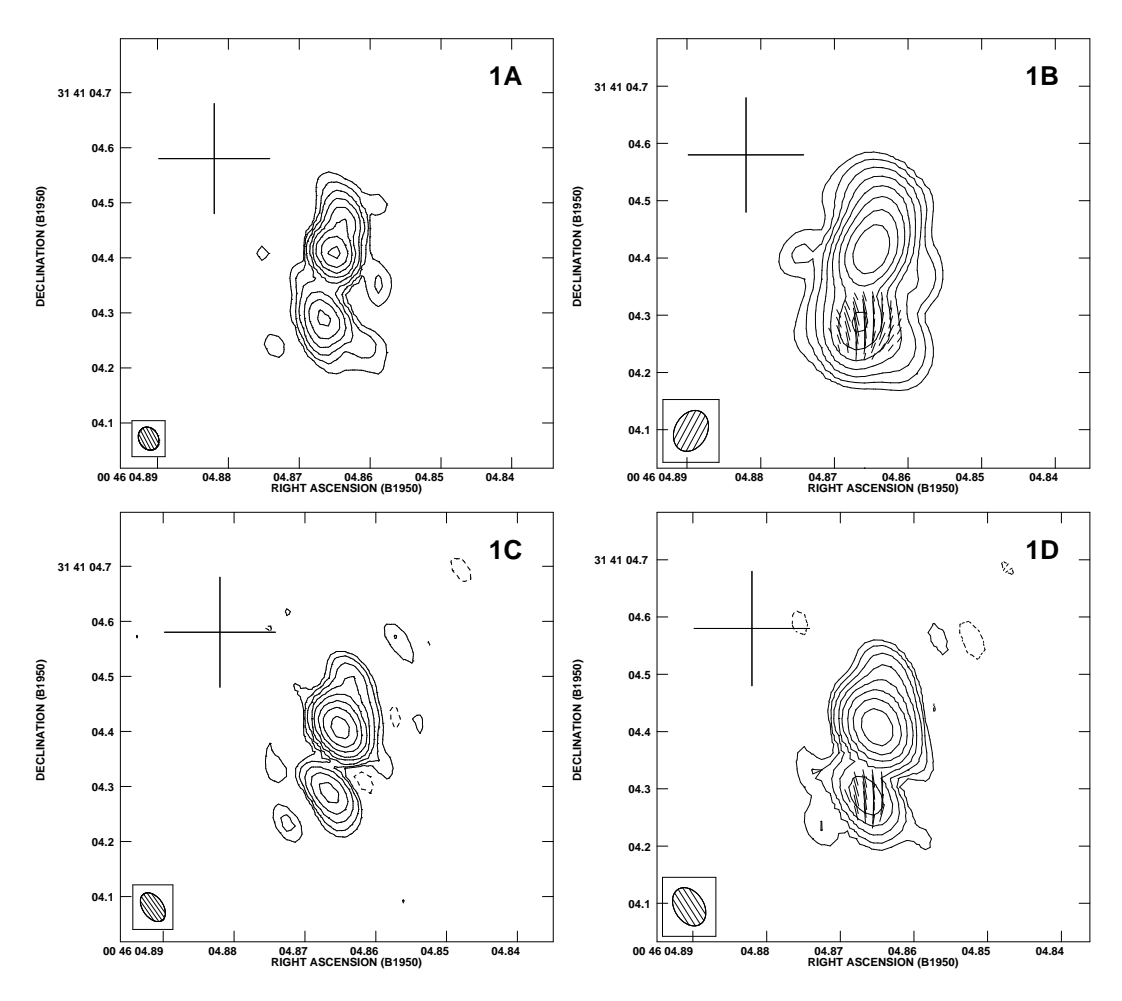


Figure 1. MERLIN maps at 5 GHz showing the 1992 uniformly-weighted map (1A), the 1992 naturally-weighted map (1B), the 1998 uniformly-weighted map (1C) and the 1998 naturally-weighted map (1D). The root-mean-square noise levels for each map (σ) , as measured in an un-CLEANed region at the edge of the field, are; 0.175 mJy/beam (1A), 0.135 mJy/beam (1B), 0.177 mJy/beam (1C) and 0.158 mJy/beam (1D). Contour levels are chosen as $3\sigma \times (-2,-1,1,2,4,8,16,32,64,128)$ for the 1992 maps and $6\sigma \times (-2,-1,1,2,4,8,16,32,64,128)$ for the 1998 maps. Crosses show the optical position of the nucleus as given by Clements (1981); the size of the cross shows the quoted positional uncertainty. Polarisation vectors with a scale of 1 mJy/beam to 0.015 arcsec are overlayed on the naturally-weighted maps.

Component	Epoch	RA (B1950)	Dec (B1950)	$\operatorname*{F_{5GHz}}_{[mJy]}$
Radio Core	1992	00 46 04.86501	31 41 04.4118	116.4
Southern		00 46 04.86653	31 41 04.2880	40.5
Radio Core	1998	00 46 04.86499	31 41 04.4075	248.1
Southern		00 46 04.86653	31 41 04.2879	31.6
Total Total	1992 1998			185.0 299.6

Table 1. The positions and flux densities of the nuclear radio components of Mrk 348 as measured with MERLIN at 5 GHz.

2.3 ISOPHOT Observations

Mrk 348 was observed at 25, 60, 90 and 170 μ m wavelengths by the Infrared Space Observatory (ISO) with the imaging

= photo-polarimeter ISOPHOT. The observations were performed in PHT03 and PHT22 (P03 and P22 hereafter) photometric modes, in chopped mode, with the same integration time on-source and on-background. The observations were carried out on the 24th of December 1996 and on the 12th of January 1997. The integration time in P03 mode was of 268 sec, and that in P22 mode was of 374 sec. P03 observations were taken with triangular chopper mode, with a throw of 60" between positions. P22 measurements were performed in rectangular chopper mode; the chopper throw was 180" between positions. The data were reduced using PIA ¶¶. Table 2 presents the results from ISO photometry. The quoted flux densities are the means of the flux densities (obtained from the several chopper measurements) and σ is the dispersion of these flux densities about the mean, not the dispersion on the mean σ/\sqrt{N} . Though for a Gaussian distribution the best estimate of the error on the mean

¶¶ PHT-Interactive Analysis. PIA is a joint development by the ESA Astrophysics Division and the ISOPHOT consortium.

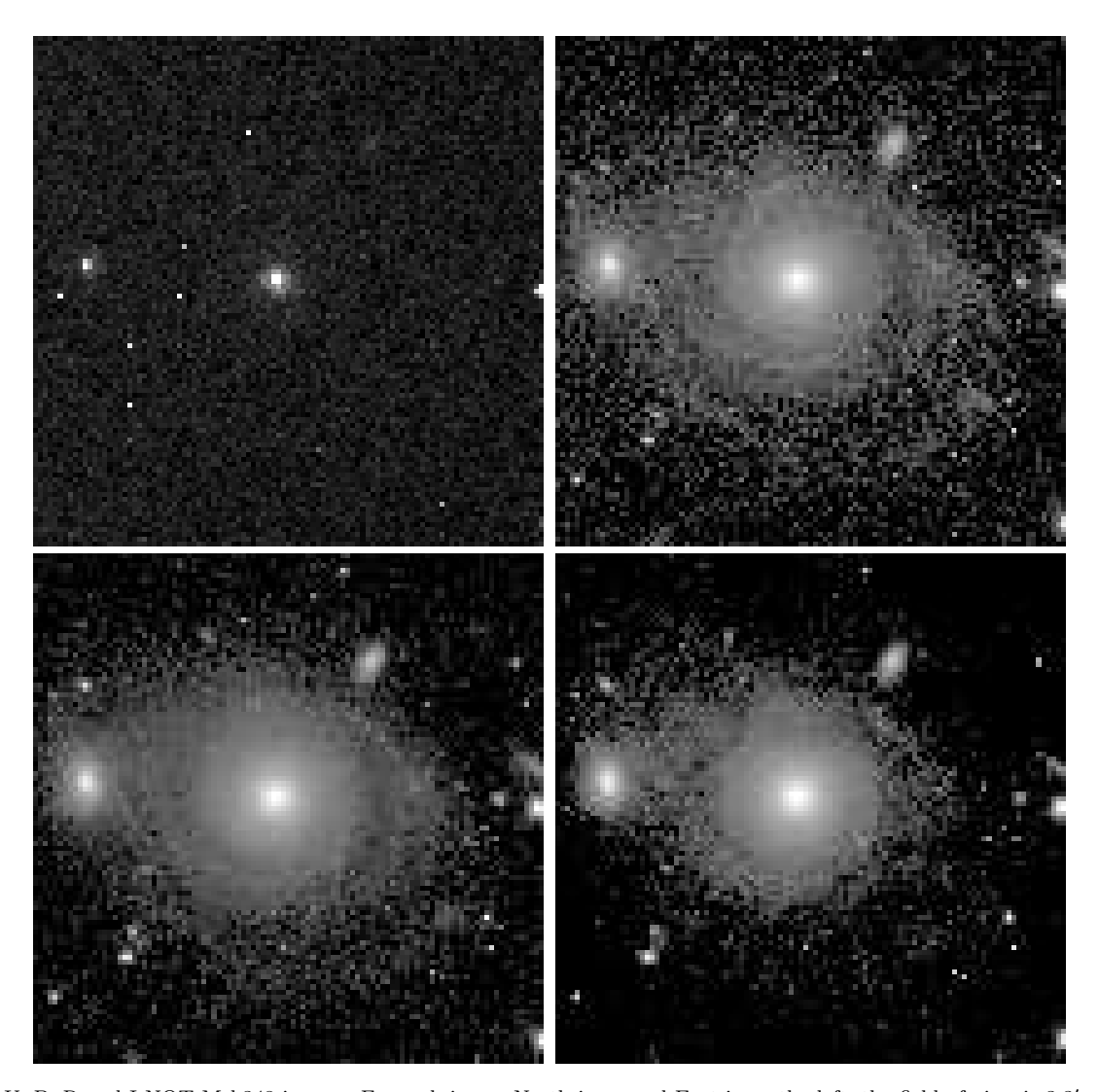


Figure 2. U, B, R and I NOT Mrk348 images. For each image North is up and East is on the left, the field of view is 3.3' × 3.3'. Top Left: U image of Mrk348. In the image we detect Mrk348 – central object – and also its eastern companion, a galaxy at the same redshift as Mrk348. Top Right: B image of Mrk348. This image reveals fine structure in the spiral arms: in the inner regions the arms are very symmetric, but the external arms show a disrupted morphology. The outermost arm ends towards the eastern companion of Mrk348. Bottom Left: R image of Mrk348. This image is similar to the B image, but we detect the more evolved red stellar population. Bottom Right: I image of Mrk348. This image is similar to R image, but here the external arm appears dimmer. Some of the faint features in the I image are due to fringing in the CCD.

is σ/\sqrt{N} , in our case we do not expect a Gaussian error distribution because the signals showed distortions due to glitches and/or long term drifts. Thus σ gives a (conservative) estimate of the significance of the measurement. Also, σ does not contain any contribution from systematic errors, as they were not quantified at the time of the data reduction. In this context, a detection means that the mean flux density is higher than 3σ , which is the case for Mrk 348 at the 4 infrared wavelengths. Mrk 348 had been detected by IRAS, and at 60 μ m there is good agreement between the IRAS (F_{IRAS}^{60\mu m}\!=\!1290\pm116 mJy) and ISOPHOT flux densities. The IRAS 100 μ m flux density (F $_{IRAS}^{100\mu m}$ =1549 \pm 201 mJy) is slightly higher than the ISO flux density at 90 μ m. Much more significant is the disagreement between the 25 μm flux densities. The 25 μm ISOPHOT flux density is approximately a factor of 3 smaller than IRAS flux density

 $(F_{IRAS}^{25\mu m}{=}835\pm25$ mJy). We suggest that this discrepancy might be explained as the sum of two effects: a) P03 measurements were performed with a 4s/chopper plateau chopper frequency, and for this setup radiation loss might occur (Haas, priv comm.) b) the chopper throw of 60" is small compared to the extent of the disk of the galaxy, and the background position is possibly contaminated by residual galaxy emission.

2.4 NOT data

In August of 1997 we obtained U, B, R and I images of Mrk 348 with the 2.6 m Nordic Optical Telescope (NOT). The observations were performed with the HiRAC camera using a 2k Loral CCD, with a field view of $3.7\times3.7~\rm arcmin^2$ and a pixel scale of 0.11 arcsec. The conditions were photomet-

F ₂₅ [mJy]	F ₆₀ [mJy]	F ₉₀ [mJy]	F ₁₇₀ [mJy]
260 (57)	1139 (330)	1108 (302)	1451 (300)

Table 2. ISO flux densities at 25, 60, 90 and 170 μ ; the rms is in parenthesis. The rms is the dispersion of the distribution of the flux densities (see text).

Aperture ["]	B [mag]	R [mag]	I [mag]
1.0	18.07	16.60	16.04
1.5	17.59	16.12	15.53
2.0	17.42	15.95	15.35
3.0	16.86	15.39	14.74
6.0	16.15	14.68	13.97
9.0	15.78	14.32	13.59
12.0	15.52	14.10	13.36

Table 3. Photometry (NOT images) of Mrk348 through different apertures.

ric with seeing ~ 0.7 arcsec throughout the observations. Standard stars from Landolt (1992) were observed and sky flats were obtained at the beginning and at the end of the nights. The data reduction was performed with IRAF. The method followed the standard procedures. The extinction coefficients were obtained through the standard stars. Airmass corrections were applied. The standard calibrations were computed to obtain the zero point magnitudes. The root mean square error of the calibrations is RMS=0.03 mag for B magnitudes, RMS=0.02 mag for R magnitudes and RMS= 0.01 mag for I magnitudes. A Point Spread Function (PSF) model was derived independently from each image, using daophot tasks. The colour image B-I was obtained by dividing the I image by the B image. To do this, the I image was shifted in position (to get a perfect matching between the 2 frames); here Galactic stars were used to obtain the registration of the frames. Then, the shifted I image was smoothed with a Gaussian filter in order to match the resolution of B image; the task gauss, which convolves an image with an elliptical Gauss function, was used for this purpose. In Figure 2 U, B, R and I images are presented. North is at the top and East is on the left. Each field of view is 3.3x3.3 arcmin² and 1" represents 327 pc in the rest frame of the source. Figure 3 presents the B-I colour image of Mrk348, where darker pixels represent bluer colours and lighter represent redder colours. Table 3 lists the B, R and I magnitudes for different apertures centered on the nucleus.

3 RESULTS

3.1 Large-scale properties

Broadband optical images of Mrk 348 have been obtained with the Hubble Space Telescope and show the structure of the inner regions of the galaxy (Malkan et al. 1998; Capetti et al. 1996). The advantage of NOT imaging is (with good seeing, as in our case) the ability to reveal structure in the

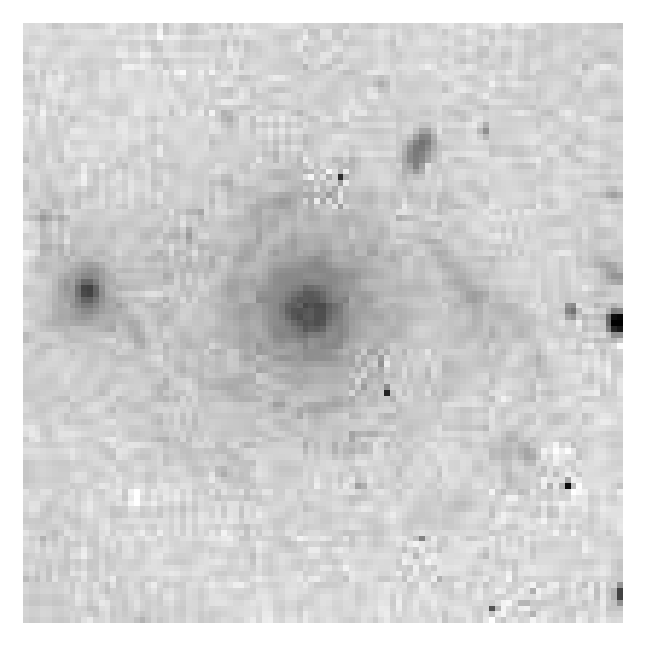


Figure 3. B-I image of Mrk348. North is up and East is left and the field of view is $3.3' \times 3.3'$. We detect a slight colour gradient in the eastern companion. The external bluish arms of Mrk348 are noticeable, as is the spiral structure in the inner regions.

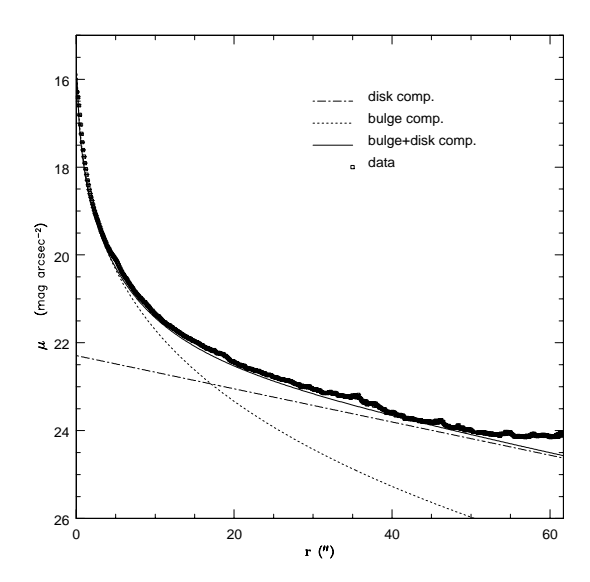


Figure 4. Bulge-disk decomposition of Mrk 348 brightness profile.

low surface brightness regions, adjacent to the HST structure. This is well demonstrated by our B image (see Figure 2) that reveals fine details of the spiral arms. Our images confirm that Mrk348 is a giant face-on spiral galaxy. From the B image we estimate an inclination angle of $\approx 20^{\circ}$. In the past the galaxy morphology has been classified as S0 (Huchra 1980), but our NOT images suggest that the morphology corresponds to a later-type. We have analysed the brightness profile of Mrk 348, which is presented in fig.4. The details of the method used to compute the profile are given in Marchã et al. (in preparation). Briefly, the profile was

6

obtained using the IRAF package ellipse, where elliptical isophotes were fitted to the galaxy image down to a surface brightness of $\mu=24.5$ mag arcsec⁻². A radial profile of the average isophotal surface brightness versus semimajor axis was then produced and model light distributions were fitted to the profile using a non-linear least-squares method. The best fit to this profile was obtained using a function that is the sum of a Vaucouleurs law and a full exponential disk, $I(r)=I(r)_{bulge}+I(r)_{disk}$ (note $\mu\sim-2.5\log$ I), where:

$$I(r)_{bulge} = I_e \ e^{-7.688} \ \frac{\left(\left(\frac{r}{r_e}\right)^{\frac{1}{4}} - 1.0\right]}{I(r)_{disk} = I_o \ e^{-\left(\frac{r}{r_o}\right)}}.$$

 r_e is defined as the radius within which half of the total light is emitted, I_e is the intensity at $r_e,\ I_o$ is the central intensity of the disk, r_o is the disk scale length. The parameters of the best fit are $r_e=2.88\pm0.01$ kpc, $\mu_e=21.44\pm0.01$ mag $\rm arcsec^{-2},\ r_o=9.39\pm0.02$ kpc, $\mu_0=22.29\pm0.01$ mag $\rm arcsec^{-2}.$ The bulge-fraction, defined as B/T = $\frac{r_e^2 I_e}{r_e^2 I_e+0.28 r_o^2 I_o}$, and related to the disk-to-bulge ratio D/B by B/T = 1/(D/B+1), is 0.4. According with Fig. 4.51 in Binney & Merriefield (1998) this value indicates that Mrk 348 lies between an Sa+ and an Sb+ type spiral galaxy. Our data demonstrate that the morphology of Mrk 348 host is indeed of a later-type than S0.

Our images show that a disrupted spiral arm ends towards the eastern companion of Mrk 348, suggesting that Mrk348 and its eastern companion form an interacting system, as first proposed by Simkin et al. (1987) primarily on the basis of radio observations of the distribution of neutral hydrogen. Also, the eastern companion shows a colour gradient, being bluer near the region where the external arm of Mrk348 seems to end (see Figure 3). If the bluish colour is the result of star forming regions, star formation could have been triggered by tidal interaction between Mrk348 and its eastern companion. Perhaps the interaction between Mrk348 and its eastern companion is responsible for triggering the nuclear activity of Mrk 348, as suggested by Simkin et al. (1987). We note, however, that the spiral structure on scales up to 30 kpc of Mrk348 is very symmetric, something that contrasts with the obviously disturbed outer structure. If the interaction is responsible for triggering the nuclear activity of Mrk 348 it is surprising that the spiral structure has managed to remain so undisturbed.

In Figure 5 we present an enlargement of the U image (Figure 2) showing the central region $(24'' \times 24'')$. A ring of continuum emission with a diameter of ~ 3.2 kpc can be seen. This ring is blue (see Figure 3) and is coincident with the H α emission regions detected by Gonzalez Delgado et al. (1997), suggesting that these are HII regions.

Motivated by the Galactic Dust Model (GDM) proposed by Malkan et al. (1998) we analysed the colour image B-I to try to identify any large-scale dusty regions. In the GDM the classification of an object as a Seyfert 1 or a Seyfert 2 depends on how the dusty regions are distributed in the inner parts of the host galaxy; if it happens that a galactic dusty region is between the observer and the central engine, then the object is classified as a Seyfert 2. We do not see any evidence of extra reddening on scales we can resolve (> 200 pc). We conclude that large-scale dusty regions are not

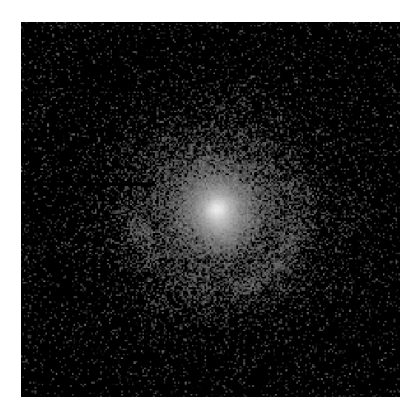


Figure 5. Central U image of Mrk348. North is up and East is left and the field of view is $24'' \times 24''$ i.e. $\sim 10 \times 10 \text{ kpc}^2$. Pseudo-colour image with logarithmic brightness scale. The ring-like distribution coincides with HII regions.

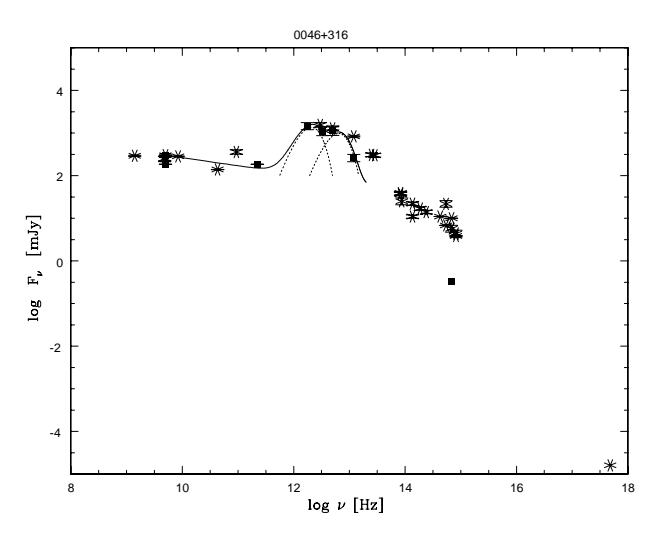


Figure 6. 0046+316: Flux densities from the literature are shown in star symbols, including IRAS data (12, 25 60 and 100 μ m). The data presented in this paper are represented by square symbols. The solid line represents the sum of a power law spectrum with two greybody spectra of temperatures \sim 20 K and \sim 62 K (each component is represented by dashed lines).

obscuring the BLR $\parallel \parallel$.

Comparison of our aperture photometry with that presented in Kotilainen & Ward (1997) suggests that the central region of Mrk 348 changed colour between 1992 and 1997 (Antón et. al., in preparation).

3.2 Properties of the central regions – The Spectral Energy Distribution (SED)

The SED, spanning wavelengths from the radio to the X-ray bands, is presented in Figure 6. Comparing the emission at radio wavelengths to that at the ISO wavelengths it is clear that the spectrum shows an excess at the infrared

Note that evidence for dust in the vicinity of the very central region has been found (see Falcke et al. 1998, Simpson et al. 1996).

wavelengths, and this excess is most naturally explained by emission by dust probably heated by the AGN. We fitted the SED between radio and infrared bands with a power-law component plus two greybody components, a cooler one with temperature ~ 20 K and a warmer one with temperature \sim 62 K. Mrk 348 has a quite flat spectrum up to the millimetre wavelengths ($S_{\nu} \sim \nu^{-0.09}$). The fact that the broadband spectrum is smooth and flat between the radio and millimetre bands suggests that the emission up to the millimetre band is synchrotron emission. The wavelength at which the non-thermal emission has a cut-off occurs at wavelengths shorter than 1.35 mm, perhaps between the sub-millimetre and far-infrared bands. The SED of Mrk 348 is very similar to that of other radio-loud objects, in which the radio emission is thought to be the result, either directly or indirectly, of the presence of a relativistic jet. We will discuss this further in the next section.

3.3 Radio Polarization

The polarisation seen in the southern component in Mrk348 is unusual as most Seyferts show little radio polarisation. This lack of polarised flux is readily explained by the depolarising effect of the ionised gas in the narrow line region(NLR), within which the radio emission is usually embedded. The fact that the southern component is 5% polarised, whereas the stronger central component is unpolarised at 6 cm (< 0.5%), can be most easily interpreted by assuming the southern component to be in front of the NLR gas, whereas the central component is embedded within it. This would be consistent with models where the southern component is associated with a jet pointing towards the observer. Although it could be argued that the lack of polarisation in the central and northern components is intrinsic, models in which the southern component is on the far side of the NLR can almost certainly be ruled out. In fact a similar situation is seen in NGC1068 (Wilson & Ulvestad 1987), where only the NW lobe shows significant polarisation, and the central and southern components are depolarised by NLR gas. This effect is analogous, albeit on a much smaller scale, to the Laing-Garrington effect (Laing 1988; Garrington et al. 1988) seen in radio galaxies.

4 DISCUSSION

One of the main reasons for studying Mrk 348 is that the observational evidence appears to point to different and mutually inconsistent scenarios. Our aim is to try and come up with a single model which is consistent with all the observational facts. This involves close examination of the evidence concerning the orientation of the AGN with respect to the line of sight and whether or not Doppler boosting is playing a dominant role in determining its observed properties. The amount of beaming has a strong bearing on the degree of radio loudness of the object; is Mrk 348 radio quiet or is it one of those (relatively rare) objects intermediate between radio-loud and radio-quiet objects?

4.1 The orientation of Mrk 348

The NOT images of Mrk 348 clearly show that the AGN is hosted by a giant nearly face-on spiral galaxy. The near circular symmetry of the galaxy is preserved down to the ring of HII regions on a scale of ~ 1 kpc. The continuum radio properties of Mrk 348 such as the flat radio spectrum continuing well into the infrared without any sign of a break, the core-dominated radio structure and the rapid radio variability (Neff & De Bruyn 1983), are all consistent with the source axis making a small angle to the line of sight to the observer. On the other hand the optical data, for example the Seyfert 2 spectrum and scattered polarized broad lines, all support a different scenario in which the axis of the AGN makes a large angle to the line of sight to the observer. The detection of strong H₂O megamaser emission in Mrk 348 by Falcke et al. (2000) might be taken as evidence to reinforce this conclusion since megamasers are almost exclusively found in Seyfert 2 galaxies which are believed to have edge-on molecular tori. However, the maser emission consisting of a single reshifted broad-line is not like that seen from the prototype edge-on disk object NGC4258 (Miyoshi et al. 1995) which has both red- and blue-shifted narrow lines. Both Peck et al. (2001) and Xanthopoulos & Richards (2001), using VLBA and MERLIN observations respectively, have reached the conclusion that the maser emission probably arises from molecular material shocked by the jet and not from a torus. Since the maser emission is only seen towards the northern VLBI jet, and it is redshifted with respect to the systemic velocity of the galaxy, the shock model suggests that the northern jet is pushing the molecular material away from us and thus implies that the northern jet is the receding one. Beyond this, it seems that the detection of H₂O maser emission in Mrk 348 places no unambiguous constraint on the orientation of the AGN axis with the line of sight to the observer.

Tran (1995) argues on the basis of his spectropolarimetry that the torus is being viewed at a low inclination. By the same argument as above this would support a scenario where the AGN axis makes a small angle to the line of sight to the observer. The evidence for ionization cones is also relevant to the orientation debate, but the data do not seem to be conclusive: a) Simpson et al. (1996) claim to see ionization cones in Mrk 348, from ground-based images, with an half-angle ~ 45 deg b) the evidence for such cones in high resolution (HST) images (Falcke et al. 1998) is, however, marginal. The VLBI results on Mrk 348 of U99 are potentially important. U99 detect a one-sided core-jet and measure subrelativistic motions in the jet with β_{app} =0.08. Again, the evidence is pointing in two different directions; the one-sided nuclear jet and the more symmetric larger-scale structure seen in the MERLIN maps, could naturally be accounted for by beaming of a relativistic nuclear jet but the sub-luminal motion fits more naturally into a picture with the jets making a larger angle to the line of sight ***. (We point out

*** There are examples of quasars with some knots showing superluminal motions, but which also have knots that are apparently stationary, e.g. 3C 395 (Lara et al. 1994). U99 believe, nevertheless, that the measured speeds represent the true jet speeds as the core and northern structures have not changed between the (two) epochs.

that a naive combination of motion of 0.08c (24 000 kms^{-1}) in the plane of the sky and the radial motion of $130 \ km s^{-1}$, deduced from the maser emission, indicates a resultant motion almost completely in the plane of the sky.) U99 suggest that the absence of a southern counterpart to the northpointing jet could be accounted for by free-free absorption by ionised gas with average density $n_e > 2 \times 10^5 \text{cm}^{-3}$, resulting in a column density of $n_H \sim 10^{23} {\rm cm}^{-2}$. This value is completely consistent with the value calculated from Xray observations (Warwick et al. 1989). We note, however, that Gallimore et al. (1999) do not detect HI absorption in front of any of the radio components and they estimate an upper limit of $n_H \sim 5 \times 10^{19} \text{cm}^{-2}$. That is, the X-ray and radio observations give very different n_H suggesting that the detected X-ray and radio-core radiation is propagating through regions with different opacities - perhaps because the bases of the radio emitting jets are located further out along the AGN axis than the X-ray emitting regions. If this is the case, the similarity of the required n_H to free-free absorb the southern component and the calculated n_H (from X-ray observations) is a coincidence.

The MERLIN polarization observations compound the confusion; attributing the polarization asymmetry to a Laing-Garrington-like effect (Laing 1988; Garrington et al. 1988) in which the near-side of the source suffers less Faraday depolarization than the far-side, argues that the southernmost component is the closest to the observer. This, incidentally, is consistent with the shock model of the maser emission put forward by Peck et al. (2001) and Xanthopoulos & Richards (2001). The U99 VLBI results, however, show only a northpointing jet, suggesting that the north-side is the approaching side of the source. This is true whether the absence of an observable southern counter-jet is a result of beaming or free-free absorption by a disk. Can this apparent conflict be resolved? It could be that in Mrk 348, instead of the obvious hypothesis that we are seeing a lobe-core-lobe structure, we are actually seeing a single one-sided jet that is moving towards the observer. In Figure 7 we present a cartoon of a possible geometrical configuration. Here, the core and "northern" components are further inside the host galaxy, and the "southern" component represents the end of the jet, further outside the host galaxy. In our model, both "northern" and "southern" components are moving towards the observer. The direction of the jet makes a small angle with the line of sight, but then bends by a small angle. Projection effects magnify the small bending, making the "southern" component appear at the south of the core. In this situation the true counter-jet might not be detected, in agreement with the U99 findings, if it is dimmed by Doppler de-boosting effects.

We summarize our conclusions about orientation as follows:

- The optical data seems to point to Mrk 348 fitting the standard model for a Seyfert 2 galaxy in which there is an obscuring structure hiding the optical AGN from view. This requires axis of the system to make a large ($\geq 45\deg$) angle to the line of sight.
- \bullet The radio core-dominated structure with small-scale one-sided jet would most naturally fit a model in which the radio jet axis makes a small angle ($\leq 10\deg$) to the line of sight and in which Doppler boosting plays an important role. However, the lack of detectable superluminal motion has led

U99 to suggest that the angle to the line of sight is not small and propose free-free absorption by a disk to account for the one-sided VLBI structure and sub-luminal motion. But the polarization asymmetry would then still remain without an obvious explanation.

- The H₂O megamaser emission adds little to the orientation debate apart suggesting that, if the motion megamaser gas is associated with that of the jet, the northerly-pointing jet is receding from us.
- Our provisional conclusion is to take the optical data at face value and assume in the subsequent discussion that the angle to the line of sight is large, and that Doppler beaming is not a dominant factor.

4.2 Mrk 348, a radio-quiet or a radio-loud object?

Radio-loud objects are generally defined as objects in which the ratio between the flux density at 5 GHz and the flux density at B band is $S_5/S_B \ge 10$ (Kellermann et al. 1989). We now consider the radio flux density. If Doppler beaming plays at most a minor role, then the observed radio flux density should be close to the intrinsic value. We now look at the optical flux density. We note that the S_5/S_B definition takes no explicit account of the dilution of the AGN light by background starlight (Browne & Marchã 1993), which can be important in the case of luminous host galaxies. This means that S_5/S_B can be an underestimate of the object's nuclear radio activity. Nevertheless, we can estimate the optical nuclear flux density of Mrk 348 at B band from the strength of the 4000Å break in a similar way to that of Marchã et al. (1996). The ratio gives $S_5/S_B=933$, a value that puts Mrk 348 in the range of radio-loud sources. On the other hand, S_B represents a lower limit to the true flux density since it is only the light which is scattered into our line of sight which is detected. In this situation the detected central continuum S_c – the fraction that is scattered towards the observer direction - represents a fraction of the true central flux S_T . We note that it would be necessary that S_c $< 0.01S_T$, i.e. a fraction of scattered light smaller than 1%, to raise S_B by a factor of 100, and put $S_5/S_B \sim 10$ (i.e. at the radio-loud/radio-quiet boundary). Nevertheless it has been found that the typical fraction of scattered light is $\sim 2\%$ (R. Fosbury in "Portugal-ESO-VLT" meeting, 2000). Thus, the ratio S₅/S_B suggests that Mrk 348 is close to, but slightly above, the radio-loud/radio-quiet boundary. In this context the combination of radio loudness and a spiral host galaxy is unusual. The above discussion assumes that Doppler beaming plays at most a minor role. But if Doppler beaming is important then Mrk 348 is intrinsically a radio-quiet object. In this context the combination of its radio-loudness and host galaxy type would fit nicely the expectation for a radio-intermediate quasar.

5 SUMMARY

Mrk348 has been classified as a Seyfert galaxy. One peculiarity of this source is that it is a relatively strong radio object hosted by a spiral galaxy, not by an elliptical galaxy. In this paper we have presented NOT U, B, R, and I images of Mrk 348. From profile fitting calculations we conclude that the

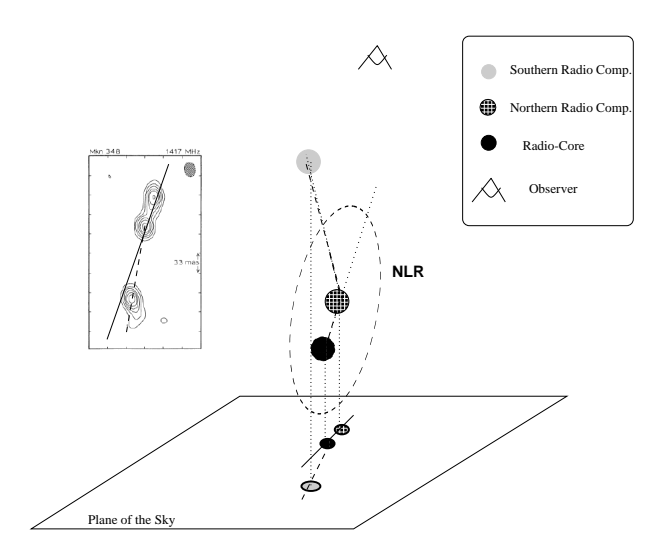


Figure 7. A possible geometrical configuration for Mrk 348, see description in the text

host galaxy of Mrk 348 is between Sa+ and Sb+ morphological type. On large scales, there is evidence that Mrk348 and its eastern companion are interacting, but based on the view of the symmetry of the inner region of Mrk348 we do not think that this interaction has triggered the Mrk 348 nuclear activity. The peculiarity of Mrk 348 comes from the SED and the polarisation seen in the southern component: both are unusual amongst radio-quiet objects. We have discussed the orientation of Mrk 348 with respect to the line of sight. The evidence points in different directions, some observations are consistent with the axis of the system to be at large ($\geq 45 \deg$) angle to the line of sight, whereas other observations are consistent if the radio jet axis makes a small (< 10 deg) to the line of sight. The orientation of Mrk 348 with the line of sight is a difficult matter to resolve and it might be that in Mrk 348 the geometry is much more complicated than a simple edge-on or face-on model. If the radio emission in Mrk348 is beamed then Mrk 348 is intrinsically a radio-quiet object. Detection of superluminal motions would be the ultimate test of such a model. Note that recently superluminal motions were detected in III Zw 2, a Seyfert galaxy that had not previously shown superluminal motions in the past (Brunthaler et al. 2000). But if the angle to the line of sight is large, and if Doppler beaming is not a dominant factor, Mrk 348 is close to, but slightly above, the radio-loud/radio-quiet boundary. In this case, the peculiarity of Mrk 348 comes from the combination of a radio-loud object harboring a spiral host galaxy.

6 ACKNOWLEDGMENTS

We thank our referee Dr Heino Falcke for constructive comments. The ISOPHOT data were reduced during a visit to the ISOPHOT Data Centre. Sónia Antón acknowledges all the support received during this visit, in particular that from Martin Haas. Sónia Antón acknowledges the European Commission, TMR Programme, Research Network Contract ERBFMRXCT96-0034 "CERES", and PRAXIS XXI Programme through the grant BD/5532/95. The NOT is operated on the island of La Palma jointly by Denmark, Finland,

Iceland, Norway, and Sweden, in the Spanish Observatorio del Roque de los Muchachos of the Instituto de Astrofisica de Canarias.

REFERENCES

Binney, J. & Merrifield, M. 1998, Galactic Astronomy (Princeton: Princeton Univ. Press)

Browne, I. W. A. & Marchã, M. J. M. 1993, MNRAS, 261, 795

Brunthaler, A., Falcke, H., Bower, G. C., Aller, M. F., Aller, H. D., Teräsranta, H., Lobanov, A. P., Krichbaum, T. P. & Patnaik, A. R. 2000, A&A, 357, L45

Capetti, A., Axon, D. J., Macchetto, F., Sparks, W. B. & Boksenberg, A. 1996, ApJ, 469, 554

Clements, E. D. 1981, MNRAS, 197, 829

Falcke, H., Sherwood, W. & Patnaik, A. R. 1996, ApJ, 471, 106

Falcke, H. , Wilson, A. S. & Simpson, C. 1998, ApJ, 502, 199

Falcke, H., Henkel, C., Peck, A. B., Hagiwara, Y., Almudena Prieto, M., & Gallimore, J. F. 2000, A&A, 358, L17

Gallimore, J. F., Baum, S. A., O'Dea, C. P., Pedlar, A. & Brinks, E. 1999, ApJ, 524, 684

Garrington, S. T., Leahy, J. P., Conway, R. G. & Laing, R. A. 1988, Nature, 331, 147

Gonzalez Delgado, R. M., Perez, E., Tadhunter, C., Vilchez, J. M. & Rodriguez-Espinosa, J. M. 1997, ApJS, 108, 155

Huchra, J. 1980, ApJL, 238, L11

Kellermann, K. I., Sramek, R., Schimdt, M., Shaffer, D. B. & Green, R. 1989, AJ, 98, 1195

Kotilainen, J. K. & Ward, M. J. 1997, A&AS, 121, 77

Laing, R. A. 1988, Nature, 331, 149

Landolt, A. U. 1992, AJ, 104, 340

Lara, L., Alberdi, A., Marcaide, J. M. & Muxlow, T. W. B. 1994, A&A, 285, 393

Malkan, M. A., Gorjian, V. & Tam, R. 1998, ApJS, 117, 25
Marchã, M. J. M., Browne, I. W. A., Impey, C. D. & Smith,
P. S. 1996, MNRAS, 281, 425

McLure, R. J., Kukula, M. J., Dunlop, J. S., Baum, S. A., O'Dea, C. P. & Hughes, D. H. 1999, MNRAS, 308, 377

Miller, J.S. & Goodrich, R.W. 1990, ApJ, 355, 456

Miyoshi, M., Moran, J., Herrnstein, J., Greenhill, L., Nakai, N., Diamond, P. & Inoue, M., 1995, Nature, 373, 127

Neff, S. G. & De Bruyn, A. G. 1983, A&A, 128, 318

Peck, A. B., Falcke, H., & Menten, K. M., 2001, in ASP Conf. Proc. Vol. 249, The Central Kiloparsec of Starbursts and AGN: The La Palma Connection, ed. J. H. Knapen, J. E. Beckman, I. Shlosman, & T. J. Mahoney (San Francisco: ASP), 321

Simkin, S. M., Su, H. -J. , Van Gorkom, J. & Hibbard, J. 1987, Science, 235, 1367

Simpson, C., Mulchaey, J. S., Wilson, A. S., Ward, M. J. & Alonso-Herrero, A. 1996, ApJL, 457, L19

Stevens, J. A., Ivison, R. J. & Jenness, T. 1997, SCUBA photometry cookbook

Tran, H. D. 1995, ApJ, 440, 578

Ulvestad, J. S., Wrobel, J. M., Roy, A. L., Wilson, A. S., Falcke, H. & Krichbaum, T. P. 1999, ApJL, 517, L81

- Unger, S. W., Pedlar, A., Neff, S. G. & De Bruyn, A. G. 1984, MNRAS, 209, 15P
- Warwick, R. S., Koyama, K., Inoue, H., Takano, S., Awaki, $H.\ \&\ Hoshi,\ R.\ 1989,\ PASJ,\ 41,\ 739$
- Wilkinson, P. N., Browne, I. W. A., Patnaik, A. R., Wrobel, J. M. & Sorathia, B. 1998, MNRAS, 300, 790
- Wilson, A. S. & Ulvestad, J. S., 1987, ApJ, 319 105
- Xanthopoulos, E. & Richards, A. M. S., 2001, MNRAS, 326,